Evidence for capillarity contributions to gecko adhesion from single spatula nanomechanical measurements

Gerrit Huber*, Hubert Mantz†, Ralph Spolenak*‡, Klaus Mecke§, Karin Jacobs†, Stanislav N. Gorb*, and Eduard Arzt*¶

*Max Planck Institute for Metals Research, Heisenbergstrasse 3, D-70569 Stuttgart, Germany; †Universität des Saarlandes, Experimentalphysik, D-66041 Saarbrücken, Germany; and §Friedrich-Alexander-Universität Erlangen–Nürnberg, Institut für Theoretische Physik, Staudtstrasse 7, D-91058 Erlangen, Germany

Edited by Jacob N. Israelachvili, University of California, Santa Barbara, CA, and approved September 13, 2005 (received for review July 27, 2005)

The hairy attachment system on a gecko's toes, consisting of one billion spatulae in the case of *Gekko gecko* [Ruibal, R. & Ernst, V. (1965) *J. Morphol.* 117, 271–294], allows it to adhere to nearly all surface topographies. The mechanistic basis for gecko adhesion has been intensely investigated, but the lowest hierarchical level, that of the spatula, has become experimentally accessible only recently. This report details measurements of the adhesion force exerted by a single gecko spatula for various atmospheric conditions and surface chemistries. Through judicious choice and modification of substrates, the short- and long-range adhesive forces are separated. In contrast to previous work [Autumn, K., Sitti, M., Liang, Y. C. A., Peattie, A. M., Hansen, W. R., Sponberg, S., Kenny, T. W., Fearing, R., Israelachvili, J. N. & Full, R. J. (2002) *Proc. Natl. Acad. Sci. USA* 99, 12252–12256], our measurements clearly show that humidity contributes significantly to gecko adhesion on a nanoscopic level. These findings are crucial for the development of artificial biomimetic attachment systems.

capillary forces | van der Waals forces | Hamaker constant

Understanding the adhesion mechanisms of biological systems is of great scientific interest (1–5) and a prerequisite for bioinspired design of adhesive systems (6, 7). The hierarchical gecko foot structure (8, 9) consists of lamellae (400–600 μm long), setae (2–10 μm wide, 100 μm long), and spatulae ($\approx$200 nm wide and long) (Figs. 1 and 2). This structure allows the animal to adhere to almost any surface topography. To date, adhesion experiments were performed on the level of a whole foot (4, 8) or of a single seta (still consisting of 100–1,000 spatulae). Recently, atomic force microscopy (AFM) was used to determine the pull-off force of even a single spatula (10). This nanomechanical technique has now been used to shed light on the mechanisms of gecko adhesion in the presence of water.

The dominant mechanism of gecko adhesion is still a matter of debate. Early studies of gecko adhesion invoked capillary forces (8, 11) due to liquid bridges, whereas a recent investigation (12) rejected the contribution of capillarity and indicated that van der Waals forces alone can give rise to the high adhesion observed. Even a monolayer of water, always present on surfaces under normal atmospheric conditions (13, 14), can significantly influence the attraction between two surfaces (15–20). In view of the recent results obtained by Autumn *et al.* (12), the controlling adhesion mechanism remains inconclusive.

Our detachment experiments on the spatular level provide additional insight. They were performed with substrates of varying degrees of hydrophilicity (contact angle) and as a function of air humidity. Because the gecko exhibits a dry adhesion system and does not produce secretion, any capillarity effects must be due to the air humidity controlled in our experiment. The method is the same as described in our previous paper (10). It is based on detachment experiments with an AFM of spatulae isolated by micromachining with a focused ion beam (Fig. 2). We report only pull-off forces of single spatulae; in cases where two spatulae detached simultaneously, the force value was halved. In total, $\approx$600 detachment measurements were performed on two setae with four spatulae at their ends.

Materials and Methods

Preparation of the Different Wafer and Glass Surfaces. Wafers of type N were supplied by Wacker Siltronic (Burghausen, Germany), and type T wafers were supplied by SilChem Handelsgesellschaft (Freiberg, Germany). The thickness of the amorphous Si oxide layers was determined by ellipsometry (EP^3, Nanofilm, Göttingen, Germany). These wafer surfaces were modified in two different ways, resulting in different wetting properties (21, 22). After the wafers were cut, the pieces were cleaned with a snow jet (a fast CO_2 jet containing CO_2 crystals; Tectra, Frankfurt/Main, Germany) to remove microscopic contamination. The samples were then treated with "piranha" solution, i.e., a 1:1 mixture of concentrated sulfuric acid and hydrogen peroxide (30%) for 30 min. They were rinsed in fresh hot Millipore water for 30 min immediately before the adhesion experiments. To produce hydrophobic substrates, they were covered with a monolayer (2.4 nm thick) of octadecyltrichlorosilane (Aldrich). Before the experiments, they were cleaned in an ultrasonic bath by ethanol, acetone, and toluene. The same cleaning procedure was done for the alkali lime silica glass coverslip.

Preparation of Single Spatulae. A single seta was sheared off a nonmoulting gecko with the aid of a needle tip. Using a binocular microscope, the isolated seta was then glued to the end of the well calibrated (23) contact-mode cantilever of an AFM (MikroMasch, Tallinn, Estonia). We used UV curing glue (Henkel Loctite Deutschland, München, Germany) to allow suitable alignment of the seta, which had to be perpendicular to the cantilever for correct force measurements. When the seta was perfectly positioned, it was fixed by curing with a UV lamp (maximum 5 min, wave length 366 nm). The specimen was then processed in a focused ion beam (FIB) microscope (FEI 200xP, Hillsboro, OR). Most terminal branches of setae were machined away to isolate a few single spatulae ($n \leq 4$). We simultaneously verified in the FIB that the glue did not spread along the stalk of the seta, which would have changed its mechanical properties. Finally, the cantilever was installed in the AFM (NanoWizard, JPK Instruments, Berlin).

Conflict of interest statement: No conflicts declared.

This paper was submitted directly (Track II) to the PNAS office.

Abbreviation: AFM, atomic force microscopy.

‡Present address: Eidgenössiche Technische Hochschule Zurich, Laboratory for Nanometallurgy, Department of Materials, Wolfgang-Pauli-Strasse 10, CH-8093 Zurich, Switzerland.

¶To whom correspondence should be addressed. E-mail: arzt@mf.mpg.de.

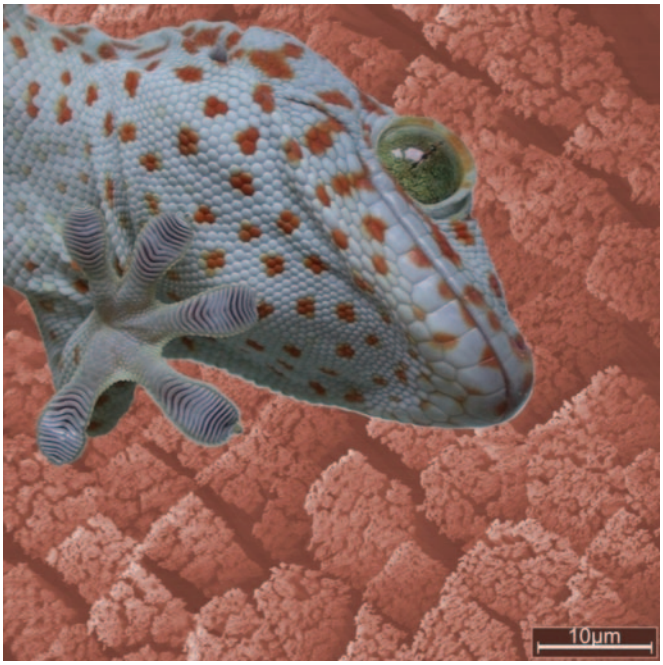

Fig. 1. The lizard *G. gecko* with one foot adhering to a glass plate (foreground) and setal structures of its attachment organs (background).

Force Measurement for a Single Spatula During Perpendicular Pull. To measure the pull-off force perpendicular to the surface, the contact silicon cantilever CSC12/Cr-Au/50 was calibrated by using the well established thermal noise method (23, 24). The force resolution of the AFM amounts to ≈70 pN. Each spatula was brought in contact by applying a vertical preload. Then the spatula was sheared by 7 μm parallel to the surface to mimic the gecko's biomechanics. The desired shearing direction was defined by the alignment of the spatulae relative to the cantilever beam. After preloading and shearing, the cantilever was vertically withdrawn while simultaneously measuring the force (512 data points per cycle). The pull-off force was defined as the minimum of the force–distance curve.

Two types of experiments were performed: First, substrates with surfaces of different contact angles for Millipore water

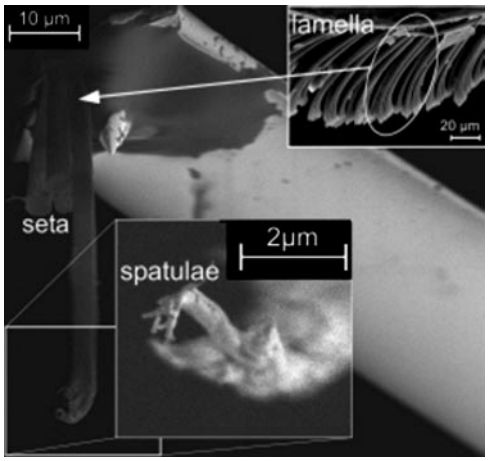

Fig. 2. SEM image of a single seta glued to an AFM cantilever. (*Insets*) Lamellar structure at lower magnification (*Upper Right*) and four single spatulae isolated at the setal tip by focused ion beam micromachining (*Lower Center*).

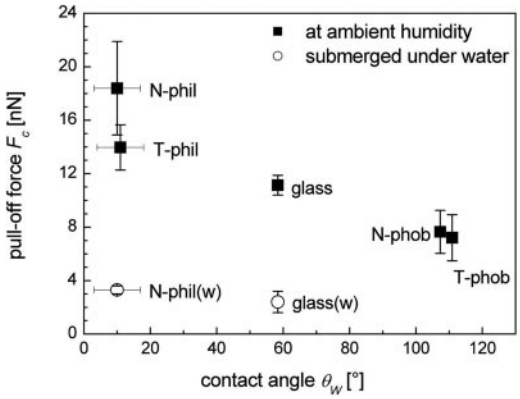

Fig. 3. Spatular pull-off force of specimen 1 vs. the contact angle θ_W of a water drop on four types of Si wafers and on glass. Wafer families N and T differ by the thickness of the top amorphous Si oxide layer. The ''phob'' type was obtained from ''phil'' type wafers by deposition of octadecyltrichlorosilane. The relative humidity during the experiment was 52%. For comparison, the pull-off forces on a glass substrate (θ_W = 58.4°) measured at comparable humidity (glass square data point taken from Fig. 4) is included. Additionally, pull-off forces while completely submerged under water [open circles labeled with glass(w) and N-phil(w)] are displayed.

were produced by varying the surface chemistry of a Si wafer by silanization. The substrate types used were wafers with different thicknesses of the top amorphous Si oxide layer (*N*, the natural ≈2-nm-thin oxide layer and T, the thermally grown thick ≈192 nm layer). The static contact angles of a sessile water drop were determined by means of the contact angle system OCAH 230 (Dataphysics Instruments, Filderstadt, Germany). When thoroughly cleaned, the Si oxide surfaces were hydrophilic, with a water contact angle of ≈10°. Both wafer types were alternatively covered by a hydrophobic monolayer of silanes (octadecyl-trichlorosilane) causing water contact angles >100°. This resulted in four types of substrates, abbreviated in the following as N-phil and N-phob as well as T-phil and T-phob. Contrary to earlier studies with different substrate materials (12), our investigation allows effects of short-range forces to be separated from those of long-range interactions: substrates exert either identical short-range but different long-range forces (N-phil and T-phil vs. N-phob and T-phob) or different short-range but similar long-range forces (N-phil and N-phob vs. T-phil and T-phob) (21, 22). The roughness of all surfaces was comparable (N type, rms <0.15 nm; T type, <0.2 nm). For comparison with our earlier data (10), a flat alkali lime silica glass (water contact angle 58.4 ± 2.7°) was also used as a substrate.

The second type of experiment involved systematic and controlled variation of air humidity. The experimental setup consisted of a commercially available AFM (NanoWizard, JPK Instruments), placed in an air-tight container. Inside the container, the humidity level was adjusted by varying the flow rate of dry nitrogen and continuously monitored by a commercially available hygrometer (testo 177-H1, Testo, Lenzkirch, Germany). Additionally, the increase in thickness of the water layer on a wafer surface was measured by ellipsometry, as a function of humidity. As an extreme case, detachment experiments were also performed for the N-phil and the glass substrates when completely submerged under fresh Millipore water.

Results

Fig. 3 shows the results of the spatular detachment measurements for the four different types of Si wafers and for the glass substrate, all at ambient temperature (25°C) and humidity (52%). Significantly higher pull-off forces were recorded for

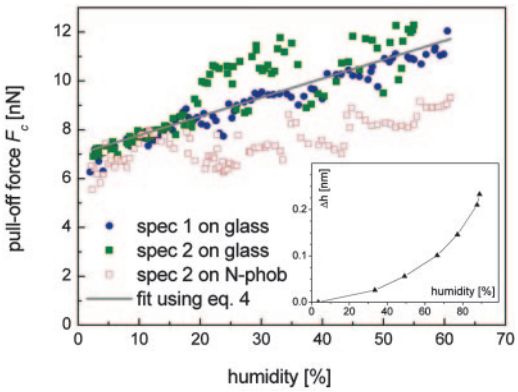

Fig. 4. Spatular pull-off forces on glass and N-phob vs. humidity at ambient temperature. The straight line corresponds to the calculations following Eq. **4**. (*Inset*) The increase Δh in water-film thickness on a Si wafer with increasing humidity as measured by ellipsometry.

both hydrophilic wafers, N-phil and T-phil, compared with the N-phob and T-phob substrates. The N-phil surface (contact angle 10 ± 7°, $n = 5$ each) gave pull-off forces of 18.4 ± 3.5 nN ($n = 60$ each). The adhesion force was slightly lower (14.0 ± 1.7 nN) on the T-phil substrate (11 ± 7°). The pull-off force was reduced by a factor of ≈2.4, to 7.7 ± 1.6 nN, on the N-phob surface (107.3 ± 0.6°). A further small decrease in adhesion was found for the T-phob substrate (110.9 ± 0.7°). Here, the adhesion force averaged 7.2 ± 1.7 nN. For the glass substrate, the pull-off forces were high when measured at ambient humidity (11.1 ± 0.7 nN). When submerged in water, much-reduced values were found, i.e., 2.4 ± 0.8 nN for glass and 3.3 ± 0.3 nN for N-phil ($n = 65$).

The detachment forces are sensitive to the presence of the octadecyl-trichlorosilane layer but not to the thickness of the oxide layer (N vs. T type). This proves that adhesion is determined by short-range forces, whereas long-range forces are insignificant. It is essential to note that detachment distances in van der Waals adhesion are typically <1 nm and independent on the strength of the force, i.e., on the Hamaker constant. Therefore, the long-range part of the attractive dispersion force is indeed irrelevant, and the pull-off force is directly proportional to the minimum value of the potential. This minimum is influenced solely by the chemical composition of few layers at the surface of the substrates.

Fig. 4 displays the spatular pull-off forces on the glass surface as a function of air humidity. Similar to the results in Fig. 3, the pull-off force values vary by up to a factor of ≈2. In virtually pure nitrogen atmosphere (≈1.5% humidity, which is the lower detection limit of the hygrometer), the adhesion force was found to be 6.4 ± 0.6 nN, $n = 10$ for specimen 1 and 7.0 ± 0.1 nN, $n = 10$ for specimen 2. With increasing humidity, the adhesion forces were found to increase in a monotonic manner; the increase was roughly linear for specimen 1 and exhibited a steeper initial slope followed by a plateau-like behavior in specimen 2. The maximum forces for both specimens were almost identical (12.1 nN for specimen 1 and 12.3 nN for specimen 2). These experiments were highly reproducible: Refilling the container with pure nitrogen resulted in the same previously measured minimum pull-off force of ≈7 nN. The same experiments conducted on the N-phob substrate resulted in a much smaller increase of adhesion force and larger scatter in the data.

Fig. 4 *Inset* shows the result of the ellipsometric thickness measurements of the water layer. At a humidity of 88%, the original film thickness on the wafer increased by ≈0.2 nm, which corresponds roughly to one additional monolayer of water. Therefore, in our experimental setup, we had at least a partial coverage of the substrate by a monolayer of water.

Discussion

The essential finding of this study is that the adhesion force of a gecko spatula rises significantly for substrates with increasing hydrophilicity (Fig. 3) and with increasing levels of humidity (Fig. 4). This striking behavior suggests that water layers between spatulae and substrates can exert an important influence on adhesion forces. Both types of experiments are essential for this conclusion, because a change in surface chemistry alone (Fig. 3) cannot distinguish between humidity effects and van der Waals effects.

It is instructive to verify whether the magnitude of the increases in adhesion force is reasonable from a theoretical point of view. A humidity effect (Fig. 4) can, in principle, be explained in two possible ways: (*i*) by standard capillarity or (*ii*) by a change of the effective short-range interaction due to adsorbed monolayers of water. The capillary force between two different surfaces, a sphere of radius R and a flat surface, may be approximately described by the standard equation (25, 26)

$$F = 2\pi R\gamma_L(\cos\theta_1 + \cos\theta_2), \qquad [1]$$

where θ_1 and θ_2 are the water contact angles on each surface, and γ_L is the liquid/vapor surface tension (72.5 mJ/m^2 for water/air). With $\theta_1 = 58°$ (for the glass substrate) and $R = 100$ nm (as a typical spatula dimension), a value of $\theta_2 = 115°$ has to be assumed in Eq. **1** to obtain a humidity-related adhesion force roughly in agreement with experiment (≈5 nN at higher humidities; see Fig. 4). The value for θ_2 is not unreasonable: sessile drop experiments performed on a gecko claw, which also consists of β-keratin, gave a value of 128 ± 4° ($n = 5$). Due to the higher roughness of the claw surface, this value can be seen as an upper bound. The smaller increase in adhesion force for the N-phob substrate in Fig. 4 cannot be explained by this approach; it is possible that subtle time-dependent surface changes due to air exposure can produce such an effect (27).

In general, such a macroscopic interpretation of the data must be considered with caution. Humidity dependence of adhesion in the presence of small amounts of water is a complex subject, which has received considerable attention over recent years e.g., refs. 28–30. Capillary forces due to liquid bridges, which can be described by contact angles and surface tensions, require a sufficient amount of water between spatula and substrate. The water amount required will depend on the contact angles of the surfaces and on the relative humidity (20). In view of the hydrophobicity of the spatula, "real" capillary condensation would be expected to occur only at relative humidities exceeding 90%, and our ellipsometry data confirm that only adsorbed monolayers of water are present. The data in Fig. 4 can be interpreted as a consequence of a change of the effective short-range interaction due to adsorbed monolayers of water between spatula and substrate. We assume that an areal fraction f of the spatula is in direct contact with the substrate. Additionally, a fraction f' of the spatula is in contact with the substrate through a monolayer of water. Assuming further that the amount of liquid is in thermal equilibrium with the vapor phase, the relative water coverage ρ is given by Langmuir's adsorption isotherm:

$$\rho = \frac{H}{H + \exp(-E/k_BT)} \approx H\cdot\exp\left(\frac{E}{k_BT}\right) \approx 1.22H, \qquad [2]$$

where H is the humidity, and E is the adsorption energy that is typically much less than the thermal energy k_BT at room temperature; above, we have assumed for the hydrophilic substrates $E = (A_wA_s)^{1/2}/16\pi \approx 0.2\,k_BT$ (where $A_w = 3.7\cdot10^{-20}$ J for

water (25), $A_s = 6.5 \cdot 10^{-20}$ J for the glass substrate). The effective Hamaker constant is expressed as

$$A_{\text{eff}} = A_{\text{dry}} f + \rho \cdot f' \cdot A_{\text{wet}}, \quad [3]$$

where A_{wet} and A_{dry} are the Hamaker constants with and without a monolayer of water. A tacit assumption inherent in Eq. **3** is that A_{dry} does not depend on humidity. The total adhesion force is given by

$$F = F_{\text{dry}}\left(1 + \rho g \frac{A_{\text{wet}}}{A_{\text{dry}}}\right) \approx F_{\text{dry}}\left(1 + 1.22 Hg \sqrt{\frac{A_w}{A_s}}\right), \quad [4]$$

where $g = f'/f$ is a geometrical factor. F_{dry} is the adhesion force of a spatula for vanishing humidity, which amounts to ≈7 nN for the glass substrate (Fig. 4). In Eq. **4**, the combining rules given in ref. 25 were used for defining A_{wet} and A_{dry}. By setting $g = 1.2$, we obtain the straight line in Fig. 4, which is in good agreement with the experimental data for the glass substrate. The lower increase for N-phob can be qualitatively explained by smaller adsorption energy, resulting in reduced water coverage ρ.

Clearly, Eq. **4** does not apply in the limit $H = 1$. In fact, an almost vanishing adhesion force under water is expected, because the Hamaker constant is drastically reduced by the high permittivity of water. This is supported by our experiments, as shown in Fig. 3. The detachment force in the presence of water is almost six times smaller than for the same experiment at ambient humidity and is independent of contact angle of the substrate. In that case, the adhesion force of a whole gecko foot would also be reduced substantially; this seems to be in agreement with circumstantial evidence from the observation of geckos when running on wet surfaces.

Conclusion

Our study demonstrates that humidity influences gecko adhesion on the spatular level. Its relative contribution depends on air humidity and substrate hydrophilicity. Such an effect can be explained, at least semiquantitatively, by considering water monolayers adsorbed between spatula and substrate. The implications of these findings have potentially high relevance in biology and engineering: studies of bioadhesive mechanisms must account for the possible influence of humidity, and capillary effects should also be optimized in the biomimetic design of artificial attachment systems.

We are grateful to J. Israelachvili (University of California, Santa Barbara) as well as C. C. Austin (Louisiana State University, Baton Rouge) for fruitful discussions. We thank D. Knebel (JPK Instruments) for script development. This study was partly supported by the BioFuture Grant of the Federal Ministry of Education and Technology, Germany (BMBF) (to S.N.G.).

1. Persson, B. N. J. (2003) *J. Chem. Phys.* **118,** 7614–7621.
2. Spolenak, R., Gorb, S. & Arzt, E. (2005) *Acta Biomater.* **1,** 5–13.
3. Stork, N. E. (1983) *J. Nat. Hist.* **17,** 829–835.
4. Irschick, D. J., Austin, C. C., Petren, K., Fisher, R. N., Losos, J. B. & Ellers, O. (1996) *Biol. J. Linn. Soc.* **59,** 21–35.
5. Autumn, K., Liang, Y. A., Hsieh, S. T., Zesch, W., Chan, W. P., Kenny, T. W., Fearing, R. & Full, R. J. (2000) *Nature* **405,** 681–685.
6. Geim, A. K., Dubonos, S. V., Grigorieva, I. V., Novoselov, K. S., Zhukov, A. A. & Shapoval, S. Y. (2003) *Nat. Mater.* **2,** 461–463.
7. Arzt, E., Gorb, S. & Spolenak, R. (2003) *Proc. Natl. Acad. Sci. USA* **100,** 10603–10606.
8. Hiller, U. (1968) *Z. Morphol. Tiere* **62,** 307–362.
9. Ruibal, R. & Ernst, V. (1965) *J. Morphol.* **117,** 271–293.
10. Huber, G., Gorb, S. N., Spolenak, R. & Arzt, E. (2005) *Biol. Lett.* **1,** 2–4.
11. Stork, N. E. (1980) *J. Exp. Biol.* **88,** 91–107.
12. Autumn, K., Sitti, M., Liang, Y. C. A., Peattie, A. M., Hansen, W. R., Sponberg, S., Kenny, T. W., Fearing, R., Israelachvili, J. N. & Full, R. J. (2002) *Proc. Natl. Acad. Sci. USA* **99,** 12252–12256.
13. Freund, J., Halbritter, J. & Hörber, J. K. H. (1999) *Microsc. Res. Technol.* **44,** 327–338.
14. Beaglehole, D. & Christenson, H. K. (1992) *J. Phys. Chem.* **96,** 3395–3403.
15. Bhushan, B. & Sundararajan, S. (1998) *Acta Mater.* **46,** 3793–3804.
16. Sugawara, Y., Ohta, M., Konishi, T., Morita, S., Suzuki, M. & Enomoto, Y. (1993) *Wear* **168,** 13–16.
17. Thundat, T., Zheng, X. Y., Chen, G. Y., Sharp, S. L., Warmack, R. J. & Schowalter, L. J. (1993) *Appl. Phys. Lett.* **63,** 2150–2152.
18. Orr, F. M., Scriven, L. E. & Rivas, A. P. (1975) *J. Fluid Mech.* **67,** 723–742.
19. Stifter, T., Marti, O. & Bhushan, B. (2000) *Phys. Rev. B* **62,** 13667–13673.
20. Bhushan, B. (1999) in *Handbook of Micro/Nanobiology* (CRC Press, Boca Raton, FL), pp. 259–261.
21. Seemann, R., Herminghaus, S. & Jacobs, K. (2001) *Phys. Rev. Lett.* **86,** 5534–5537.
22. Seemann, R., Herminghaus, S. & Jacobs, K. (2001) *J. Phys.-Condens. Mat* **13,** 4925–4938.
23. Hutter, J. L. & Bechhoefer, J. (1993) *Rev. Sci. Instrum.* **64,** 1868–1873.
24. Butt, H. J. & Jaschke, M. (1995) *Nanotechnology* **6,** 1–7.
25. Israelachvili, J. N. (1992) in *Intermolecular & Surface Forces* (Academic, London), pp. 186–192.
26. Xuefeng, T. & Bhushan, B. (1996) *J. Phys. D* **29,** 163–178.
27. Leckband, D., Chen, Y.-L., Israelachvili, J., Wickman, H. H., Fletcher, M. & Zimmerman, R. (1993) *Biotechnol. Bioeng.* **42,** 167–177.
28. Jang, J., Schatz, G. C. & Ratner, M. A. (2004) *J. Chem. Phys.* **120,** 1157–1160.
29. Xiao, X. & Qian, L. (2000) *Langmuir* **16,** 8153–8158.
30. He, M., Blum, A. S., Aston, D. E., Buenviaje, C., Overney, R. M. & Luginbuhl, R. (2001) *J. Chem. Phys.* **114,** 1355–1360.